

# Excitations of a Bose-Einstein Condensate at Non-Zero Temperature: A Study of Zeroth, First, and Second Sound

D.M. Stamper-Kurn, H.-J. Miesner, S. Inouye, M.R. Andrews, and W. Ketterle

*Department of Physics and Research Laboratory of Electronics,  
Massachusetts Institute of Technology, Cambridge, MA 02139*

(Submitted to Phys. Rev. Lett. January 25, 1998)

Collective excitations of a dilute Bose gas were probed above and below the Bose-Einstein condensation temperature. The temperature dependencies of the frequency and damping rates of condensate oscillations indicate significant interactions between the condensate and the thermal cloud. Hydrodynamic oscillations of the thermal cloud were observed, constituting first sound. An antisymmetric dipolar oscillation of the thermal cloud and the condensate was studied, representing the bulk flow of a superfluid through the normal fluid. The excitations were observed *in situ* using non-destructive imaging techniques.

PACS numbers: 03.75.Fi, 05.30.Jp, 51.40.+p, 67.90.+z

Bose-Einstein condensation in dilute atomic gases [1–3] has provided a testing ground for well-developed many-body theories of quantum fluids. Many studies have focused on the collective excitations of such gases, which fully describe their dynamics and transport properties such as superfluidity. Experiments have studied low-lying collective excitations over a range of temperatures [4–6] and higher-lying modes [7]. Zero-temperature findings have agreed well with theoretical predictions based on a mean-field description of the weak interatomic interactions [8–10]. However, the behavior at non-zero temperature, which involves interactions between the condensate and the thermal cloud, is not fully understood, pointing to the need for new theoretical developments.

The physical nature of collective excitations depends on the hierarchy of three length scales: the wavelength of the excitation  $\lambda$ , the healing length  $\xi$  which is determined by the condensate density, and the mean-free path  $l_{\text{mfp}}$  for collisions between the collective excitation and other excitations which comprise the thermal cloud. The collisionless regime, defined by  $\lambda \ll l_{\text{mfp}}$ , occurs at zero temperature and for low densities of the thermal cloud. There, free-particle excitations are obtained at short wavelengths ( $\lambda \ll \xi$ ) while phonon-like excitations known as zeroth sound are obtained at long wavelengths ( $\lambda \gg \xi$ ). For excitations where  $\lambda$  is comparable to the size of the sample, this latter condition defines the Thomas-Fermi regime. Experiments have been performed either in the limit of zeroth sound excitations [5,7], or intermediate to the two limits [4,6].

At higher thermal densities, when  $\lambda \gg l_{\text{mfp}}$  collective excitations become hydrodynamic in nature, and one expects two phonon-like excitations known as first and second sound. The presence of two hydrodynamic modes is similar to the case of superfluid  $^4\text{He}$ . However, while in superfluid  $^4\text{He}$  second sound is an entropy wave with no density oscillation, in a dilute Bose gas both first and second sound describe density waves. First sound, which

is defined as having the larger speed of sound, involves mainly the thermal cloud, whereas second sound is similar in character to zeroth sound and is confined mainly to the condensate [11,12].

In this Letter, we study collective excitations at non-zero temperature, and extend earlier work [6] in several ways. First, we study zeroth sound condensate oscillations entirely in the Thomas-Fermi regime. In contrast, results of the earlier study were complicated by the transition of the condensate from the Thomas-Fermi to the free-particle regime with increasing temperature. Second, near the critical temperature we approached the hydrodynamic limit and observed the onset of hydrodynamic excitations analogous to first sound. Finally, we observed a new out-of-phase dipolar oscillation of the condensate and the thermal cloud, analogous to the out-of-phase second sound mode in liquid helium [12].

The excitations were probed generally in three steps. First, as described in previous work [13], we produced a magnetically confined, ultracold gas of atomic sodium in a well-determined equilibrium state. This state was controlled by adjusting the final frequency  $\nu_{\text{rf}}$  used in the rf evaporation by which the clouds were cooled. The clouds were cigar-shaped with weak confinement along one direction (axial), and tight confinement in the other two (radial). Second, the cloud was manipulated with either time-dependent magnetic fields or off-resonant light to excite low-lying collective modes. Finally, the cloud was allowed to oscillate freely and probed *in situ* with repeated, non-destructive phase-contrast imaging [7].

To accurately characterize the magnetic trapping potential, we excited center-of-mass oscillations of the cloud in the axial direction by sinusoidally varying the position of the trap center. By observing the subsequent motion of the cloud, we measured the axial trapping frequency as  $\nu_z = 16.93(2)$  Hz, while the radial frequency was estimated to be 230 Hz based on earlier measurements.

The  $m = 0$  quadrupolar modes of the condensate and the thermal cloud [5] were excited by a 5-cycle pulsed

modulation of the axial magnetic field curvature. Condensate oscillations were produced with driving frequencies of 25 – 27 Hz, while the thermal cloud was excited at about 30 Hz. As shown in Figure 1, the most prominent feature of the condensate oscillations was the change in the axial length. Data were evaluated for oscillations with a relative amplitude of about 10% [14].

The oscillations of each cloud were probed with 22 non-destructive images: one before the excitation to characterize the initial conditions, and three groups of 7 images during the oscillation. The three groups were separated by a delay time which was varied between 1 and 200 ms according to the damping time of the oscillation. This method of probing gave highly accurate single-shot measurements of oscillation frequencies and damping rates, allowed data to be collected efficiently, and overcame the additional fluctuations introduced when combining data from observations on several clouds.

Phase-contrast images were analyzed by fitting the observed column densities  $\tilde{n}(r, z)$  [15] with the function

$$\begin{aligned} \tilde{n}(r, z) = h_c \max & \left( 0, 1 - \frac{r^2}{(l_r/2)^2} - \frac{z^2}{(l_z/2)^2} \right)^{3/2} + \\ & h_t g_2 \left( \exp\left(-\frac{r^2}{2(\sigma_r/2)^2} - \frac{z^2}{2(\sigma_z/2)^2}\right) \right). \end{aligned} \quad (1)$$

Here,  $r$  and  $z$  are the radial and axial coordinates, respectively, while  $l_r$  and  $l_z$  are the lengths of the condensate and  $\sigma_r$  and  $\sigma_z$  are the rms diameters of the thermal cloud. The function  $g_2$  is defined by  $g_2(x) = \sum_{i=1}^{\infty} x^i / i^2$ . Eq. 1 is motivated by a simple model of the mixed cloud: a mean-field dominated condensate amid a saturated non-interacting non-condensed Bose gas. Yet, since all quantities were allowed to vary independently, Eq. 1 is an almost model-independent parametrization of a bimodal distribution:  $l_z$  is determined from the cusps of the bimodal distribution, and  $\sigma_z$  from the thermal tails.

The initial conditions for the oscillation were characterized by the total number of atoms  $N$ , the temperature  $T$ , and the chemical potential  $\mu$ .  $N$  was obtained by integrating the column density, while  $T$  and  $\mu$  were determined from the fits by  $k_B T = \pi^2 m \nu_z^2 \sigma_z^2$  and  $\mu = \pi^2 m \nu_z^2 l_z^2$ , where  $k_B$  is Boltzmann's constant. For mixed clouds,  $T$  was determined by fitting the thermal wings alone. The initial conditions (Fig. 2) were varied by adjusting  $\Delta\nu_{\text{rf}} = \nu_{\text{rf}} - \nu_{\text{bot}}$  where  $\nu_{\text{bot}}$  is the resonant rf frequency at the bottom of the magnetic trap which remained constant within 20 kHz. The Bose-Einstein condensation transition was observed at  $T = 1.7 \mu\text{K}$  with about  $80 \times 10^6$  atoms. The temperature varied linearly with  $\Delta\nu_{\text{rf}}$ , with a slope of  $3.5 \mu\text{K}/\text{MHz}$ , and was measurable down to  $0.5 \mu\text{K}$ . Reliable determinations of  $l_z$  (and  $\mu$ ) were obtained only below  $\Delta\nu_{\text{rf}} = 350 \text{ kHz}$ . For low  $\Delta\nu_{\text{rf}}$ ,  $\mu/k_B \simeq 380 \text{ nK}$ , corresponding to a condensate of  $15 \times 10^6$  atoms with a maximum density of  $n_0 = 3.8 \times 10^{14} \text{ cm}^{-3}$  using  $\mu = n_0 \cdot 4\pi\hbar^2 a/m$  with the

scattering length  $a = 2.75 \text{ nm}$ .

The lengths  $l_z$  and  $\sigma_z$  were fit independently to decaying sinusoidal functions of time. We thus determined the frequency and damping rate of two distinct oscillations. We observed no evidence for coupling between the oscillations in  $l_z$  and in  $\sigma_z$ , allowing one to consider the excitations as nearly isolated oscillations of the thermal cloud and of the condensate, respectively.

The thermal cloud oscillated at a frequency of about  $1.75 \nu_z$  with a damping rate of about  $20 \text{ s}^{-1}$ , both above and below the transition temperature (Fig. 3). The observed frequency  $\nu$  is between the predictions of  $\nu = 2\nu_z$  in the collisionless limit, and of  $\nu = 1.55 \nu_z$  in the hydrodynamic limit [16]. The damping rate is predicted to vanish in both the collisionless and hydrodynamic limits, and to reach a broad maximum of  $\sim 1.4 \nu$  when  $\nu$  is between its two limiting values [17], in agreement with our observation. The collisional mean-free path  $l_{\text{mfp}} \simeq (n_T \sigma)^{-1} = 96 \mu\text{m} \times (T/\mu\text{K})^{-3/2}$  using the peak density of the thermal cloud  $n_T = 2.612 (mk_B T / 2\pi\hbar^2)^{3/2}$ , and a collisional cross section  $\sigma = 8\pi a_{\text{sc}}^2$ . Around the transition temperature, we find  $\sigma_z \simeq 8l_{\text{mfp}}$ . This comparison of length scales, the observed frequency shift away from  $2\nu_z$ , and the high damping rate all demonstrate that the collective behavior of the thermal cloud is strongly affected by collisions. Thus, the thermal oscillations which we observe indicate the onset of hydrodynamic excitations, i.e. first sound. However, the pure hydrodynamic limit, characterized by low damping, would only be reached for even larger clouds.

We studied the quadrupolar condensate oscillations in greater detail. Typical oscillation data (Fig. 4.) demonstrate that the oscillation has a slightly lower frequency and is damped more rapidly at high temperature than at low temperature. At low-temperatures, the condensate oscillation frequency approached a limiting value of  $1.569(4) \nu_z$ , close to the zero-temperature, high-density prediction of  $1.580 \nu_z$  [9]. The slight difference between these values may be due to non-zero temperature effects even for small  $\Delta\nu_{\text{rf}}$ . At higher temperatures, the frequency drops below the low-temperature limit. This trend might be explained by the simple non-zero temperature application of Bogoliubov theory [18], in which the condensate oscillates in a combination of the external trapping potential  $U(r, z)$  and a mean-field potential exerted by the (static) thermal cloud. Considering a thermal density  $n_T \propto e^{-U(r, z)/k_B T}$ , one can estimate that the mean-field potential shifts the collective excitation frequencies downward by as much as 5%. This shift, which scales as  $a/\lambda_{\text{dB}}$  where  $\lambda_{\text{dB}}$  is the thermal deBroglie wavelength, is consistent in magnitude with those which we observed.

Damping rates for the condensate oscillations varied strongly with temperature, rising from a low-temperature limit of about  $2 \text{ s}^{-1}$  to as much as  $15 - 20 \text{ s}^{-1}$  at high temperatures. Recent treatments based on Landau

damping [19–21] provide qualitative agreement with our findings. A quantitative prediction for these damping rates [21] could not be checked because our data were collected for  $k_B T \leq 6\mu$ , where the high-temperature prediction might not be applicable, while the inability to measure  $T$  for low  $\Delta\nu_{\text{rf}}$  prevents a comparison at low temperatures.

Can the condensate oscillations be considered to be second sound? A comparison of length scales —  $l_z \simeq 4l_{\text{mfp}}$  at high-temperatures — suggests that hydrodynamic effects may already be present. However, there are no theoretical predictions regarding the transition from zeroth to second sound with which to compare our data. In future experiments with larger condensates, the signature of this cross-over may appear in the damping rate of the oscillations, which should decrease again at high-temperatures as one reaches the hydrodynamic limit.

To further probe the interaction between the thermal cloud and the condensate, we studied an excitation of a different symmetry: the rigid-body, out-of-phase motion of the condensate and the thermal cloud in the harmonic trapping potential [12]. At temperatures where the condensate fraction approaches 50%, both components should participate equally in this motion. This mode is analogous to second sound in liquid helium, where the superfluid and the normal fluid undergo out-of-phase density oscillations of equal magnitude.

We excited this mode by using off-resonant, blue-detuned laser light, which repels atoms due to the AC Stark shift [2,7,22]. We produced a 3  $\mu\text{K}$ -high repulsive potential by focusing 40 mW of light at 514 nm to an elongated spot with  $1/e^2$  half-widths of about 12  $\mu\text{m}$  and 100  $\mu\text{m}$ . After a partly condensed cloud was formed, the light was turned on and directed at the edge of the cloud, where it overlapped only with the thermal cloud. By tilting a motorized mirror, the laser beam was steered toward and then away from the center of the cloud, thereby pushing the thermal cloud in the axial direction while not directly affecting the condensate. The light was then turned off, and the cloud allowed to freely oscillate.

The position of the center-of-mass of the condensate (Fig. 5a) was monitored with repeated phase-contrast images, and data from several repetitions of the experiment were collected with a variable delay between excitation and probing. The condensate motion was initially slow, and then grew to an asymptotic sinusoidal oscillation, corresponding to the in-phase motion of the entire cloud (condensate plus thermal cloud) in the magnetic trap at the trapping frequency  $\nu_z$ . By subtracting the undamped center-of-mass motion of the entire cloud, we isolated the antisymmetric oscillation of the condensate and the thermal cloud (Fig. 5b).

The frequency of the asymmetric dipole mode of 17.26(9) Hz was significantly lower than the trapping frequency which was  $\nu_z = 18.04(1)$  Hz at that time. This  $\sim 5\%$  frequency shift is again clear evidence of the in-

teraction between the thermal cloud and the condensate. The motion exhibited in this oscillation can be regarded as the bulk flow of a superfluid through the surrounding normal fluid. Therefore, the damping which we observe directly measures the dissipation of superfluid flow. By varying the amplitude of the oscillation, one can study this dissipation as a function of velocity, and obtain more detailed information about the superfluidity of Bose-Einstein condensed gases. Further, the motion we observed, in which the condensate is driven by the moving thermal cloud, cannot be described by recent theories which assume a stationary thermal cloud [18], and requires more sophisticated treatments [20].

In conclusion, we have studied the collective excitations of a dilute Bose gas at non-zero temperatures in the Thomas-Fermi limit, and near the hydrodynamic regime. The hydrodynamic oscillation of the thermal cloud, corresponding to first sound, was indicated by measurements both above and below the Bose-Einstein condensation transition. The accurately determined frequency shift of the quadrupole oscillations away from their zero-temperature limit and of the antisymmetric oscillation away from the trap frequency are measures of the forces exerted by the condensate and the thermal cloud on one another. The damping of these modes sheds light on the dissipation of superfluid flow.

We are grateful to Allan Griffin, Jason Ho, Dan Rokhsar, and Sandro Stringari for insightful discussions, and to Dallin Durfee for experimental assistance. This work was supported by the Office of Naval Research, NSF, Joint Services Electronics Program (ARO), and the David and Lucile Packard Foundation. D.M.S.-K. acknowledges support from NSF Graduate Research Fellowships.

- 
- [1] M. H. Anderson *et al.*, Science **269**, 198 (1995).
  - [2] K.B. Davis *et al.*, Phys. Rev. Lett. **75**, 3969 (1995).
  - [3] C.C. Bradley, C.A. Sackett, and R.G. Hulet, Phys. Rev. Lett. **78**, 985 (1997), see also: C.C.Bradley *et al.*, Phys. Rev. Lett. **75**, 1687 (1995).
  - [4] D.S. Jin *et al.*, Phys. Rev. Lett. **77**, 420 (1996).
  - [5] M.-O. Mewes *et al.*, Phys. Rev. Lett. **77**, 988 (1996).
  - [6] D.S. Jin *et al.*, Phys. Rev. Lett. **78**, 764 (1997).
  - [7] M.R. Andrews *et al.*, Phys. Rev. Lett. **79**, 553 (1997).
  - [8] M. Edwards *et al.*, Phys. Rev. Lett. **77**, 1677 (1996).
  - [9] S. Stringari, Phys. Rev. Lett. **77**, 2360 (1996).
  - [10] E. Zaremba, Phys. Rev. A **57**, 518 (1998); G.M. Kavoulakis and C.J. Pethick, preprint cond-mat/9710130.
  - [11] T.D. Lee and C.N. Yang, Phys. Rev. **113**, 1406 (1959); A. Griffin, *Excitations in a Bose-Condensed Liquid* (Cambridge University Press, Cambridge, 1993) and refs.

- therein; A. Griffin and E. Zaremba, Phys. Rev. A **56**, 4839 (1997); V.B. Shenoy and T.-L. Ho, preprint cond-mat/9710274. Several authors note that the character of first and second sound is interchanged at very low temperatures.
- [12] E. Zaremba, A. Griffin, and E. Nikuni, preprint cond-mat/9705134.
  - [13] M.-O. Mewes *et al.*, Phys. Rev. Lett. **77**, 416 (1996).
  - [14] At a relative amplitude of  $\approx 10\%$ , the condensate oscillation frequency approached its low amplitude limit while the frequency rose by as much as 1 Hz at an amplitude of 50%.
  - [15] A phase-contrast image gives the optical phase  $\phi$  accrued by off-resonant light passing through a dense medium. For our probe detuning, wavelength, and polarization, the column density  $\tilde{n} = \phi \cdot 6.2 \times 10^{11} \text{ cm}^{-2}$ .
  - [16] A. Griffin, W.-C. Wu and S. Stringari, Phys. Rev. Lett. **78**, 1838 (1997); Yu. Kagan, E.L. Surkov and G.V. Shlyapnikov, Phys. Rev. A **55**, R18 (1997).
  - [17] G.M. Kavoulakis, C.J. Pethick, and H. Smith, preprint cond-mat/9710130.
  - [18] D.A.W. Hutchinson, E. Zaremba, and A. Griffin, Phys. Rev. Lett. **78**, 1842 (1997); R.J. Dodd, M. Edwards, C.W. Clark, and K. Burnett, Phys. Rev. A **57**, R32 (1998).
  - [19] W.V. Liu, Phys. Rev. Lett. **79**, 4056 (1997); L.P. Pitaevskii and S. Stringari, preprint cond-mat/9708104;
  - [20] S. Giorgini, preprint cond-mat/9709259.
  - [21] P.O. Fedichev, G.V. Shlyapnikov, and J.T.M. Walraven, preprint cond-mat/9710128.
  - [22] M.R. Andrews *et al.*, Science **275**, 637 (1997).

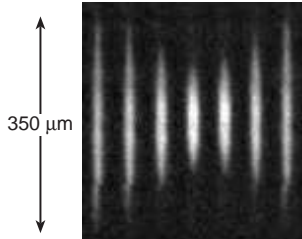


FIG. 1. *In situ* images of the  $m = 0$  quadrupolar condensate oscillation. A Bose-Einstein condensate with no discernible thermal component was imaged every 5 ms by phase-contrast imaging. The evident change in the axial length of the condensate was used to characterize the oscillation. Final data were evaluated for smaller oscillation amplitudes.

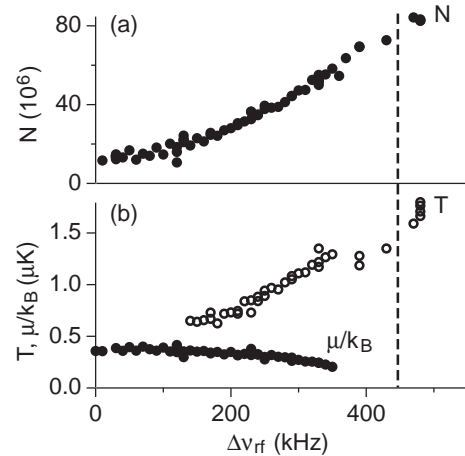


FIG. 2. Characterization of the trajectory across the Bose-Einstein condensation transition. The total number  $N$  (a) was determined by summing over the observed column densities. The temperature  $T$  (b, open circles) and chemical potential  $\mu$  (b, closed circles) were determined from fits to the data. These are plotted against  $\Delta\nu_{\text{rf}}$ . The dashed line indicates the observed transition temperature.

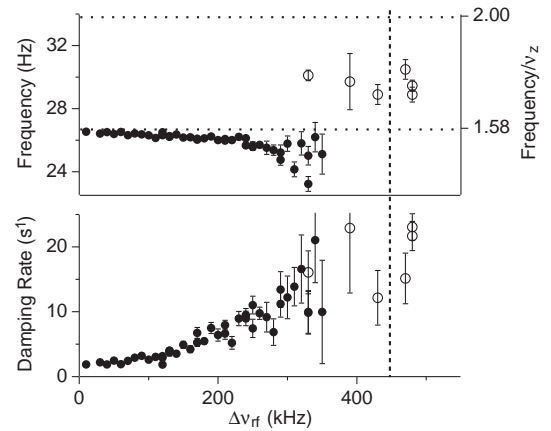


FIG. 3. Temperature dependent frequency and damping rates of  $m = 0$  quadrupolar collective modes. Points show measurements for oscillations of the thermal cloud (open circles) and condensate (closed circles). Horizontal dotted lines indicate the free-particle limit of  $2 \nu_z$  and the zero-temperature condensate oscillation limit of  $1.580 \nu_z$ . The vertical dashed line marks the observed transition temperature.

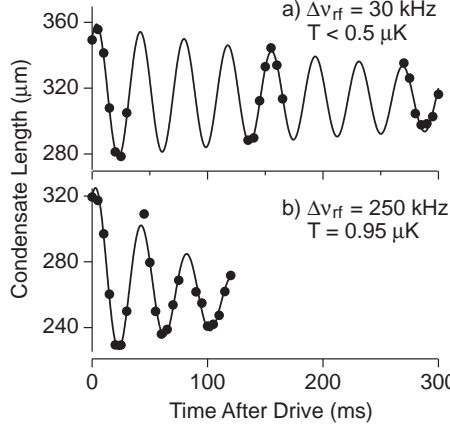


FIG. 4. Damped quadrupolar condensate oscillations at low (a) and high (b) temperature. Points show the axial condensate length determined from fits to phase-contrast images. Lines are fits to a damped sinusoidal oscillation with a downward slope. This slope accounted for heating during the oscillation. The oscillation at high temperature has a slightly lower frequency, and is damped more rapidly than at low temperature.

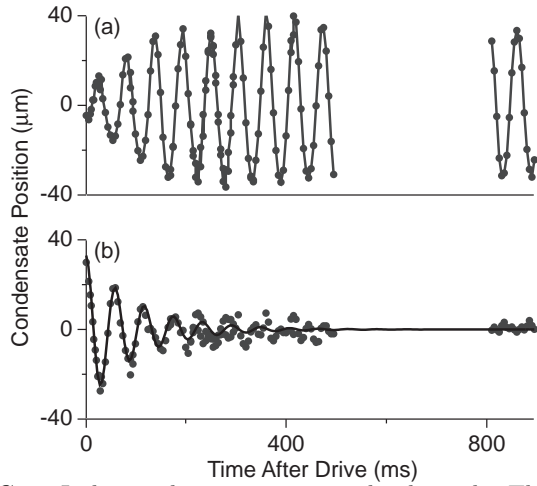


FIG. 5. Isolating the antisymmetric dipole mode. The center-of-mass of the condensate in the trap (a) was monitored after the selective displacement of the thermal cloud with a far-detuned laser beam. The oscillation of the condensate relative to the center-of-mass of the entire sample (b) occurred at a frequency below the trap frequency with a damping rate of  $9(1)\text{s}^{-1}$ . The initial conditions were  $T = 1\mu\text{K}$ ,  $\mu/k_B \simeq 200\text{nK}$ , and  $N = 40 \times 10^6$ .